

MAPPING CRATER DENSITY VARIATION ON COPERNICAN EJECTA BLANKETS: EVIDENCE FOR AUTO-SECONDARY CRATERING AT TYCHO AND ARISTARCHUS. M. Zanetti¹, A. Stadermann¹, T. Krüger², C. van der Bogert³, H. Hiesinger³, B. Jolliff¹, ¹Department of Earth and Planetary Sciences & McDonnell Center for the Space Sciences, Washington University in St Louis; ²Albert-Ludwigs-Universität, Freiburg, Germany. ³Institut für Planetologie, Westfälische Wilhelms - Universität Münster, Germany. (Michael.Zanetti@wustl.edu)

Introduction: The continuous ejecta blanket of a crater (located within ~ 1 crater radius from the rim) is completely resurfaced by the emplacement of the ejecta curtain and by ballistic sedimentation [e.g. 1,2]. It follows that the size-frequency distribution (SFD) of small craters on continuous ejecta deposits should represent the primary impactor flux since the time of parent crater formation. However, measurements on individual units (e.g. melt ponds and flows) within the continuous ejecta of a single parent crater have shown that the SFD and derived absolute model age can vary greatly depending on count area size, distance from the crater rim, target properties, topographic effects, image resolution, diameter range of craters evaluated, external secondary cratering, and potentially auto-secondary cratering (i.e. late-arriving ejecta fragments from the parent impact that form craters on the recently emplaced ejecta surface) [3-9]. Here we present evidence based on crater population density, irrespective of crater diameter, from the ejecta blankets of Tycho and Aristarchus that auto-secondary cratering occurs on continuous ejecta deposits. These results have implications for both the impact cratering process (how are auto-secondaries produced?) and cratering statistics (auto-secondaries may have been included in estimates for cratering rates during the Copernican epoch).

Methods: Craters >50 m in diameter were counted on continuous ejecta deposits using Kaguya Terrain Camera [10] and LROC NAC [11] imagery. At Aristarchus (42 km diameter), craters within 20 km of the crater rim were counted on the entire continuous blanket. At Tycho (82 km diameter), craters within 40 km of the rim in the eastern and western quarters of the continuous ejecta were counted. All craters counted superpose the ejecta blanket. Additionally, measurements were done on mapped impact melt ponds and flows [12, 13]. Counts were done using CraterTools [14] in ArcGIS, and statistics were compiled using CraterStats [15], using production and chronology functions from [16]. Point density maps were created using standard tools in ESRI ArcGIS 10.1 [17].

Results: The size-frequency distribution of craters at Tycho for the entire count areas differ little from east to west (East $N(1)=6.07 \times 10^{-5}$, $\text{area}=3.91 \times 10^3 \text{ km}^2$; West $N(1)=5.52 \times 10^{-5}$, $3.87 \times 10^3 \text{ km}^2$), equating to an absolute model age (AMA) of 65.9 ± 1.4 and 72.4 ± 1.5 , respectively. However, the density of craters does increase with distance from the rim of Tycho (Fig. 1a).

Subdividing the count areas based on the observed crater density shows that low density regions have 3.9 times fewer craters than high density regions. Melt surfaces at Tycho have even lower values ($N(1)=3.4 \times 10^{-5}$, $\text{area}=2.72 \times 10^2 \text{ km}^2$, $\text{AMA}=40.6 \pm 2.2$). Crater density ranges from 0.3 to 3.7 craters/ km^2 .

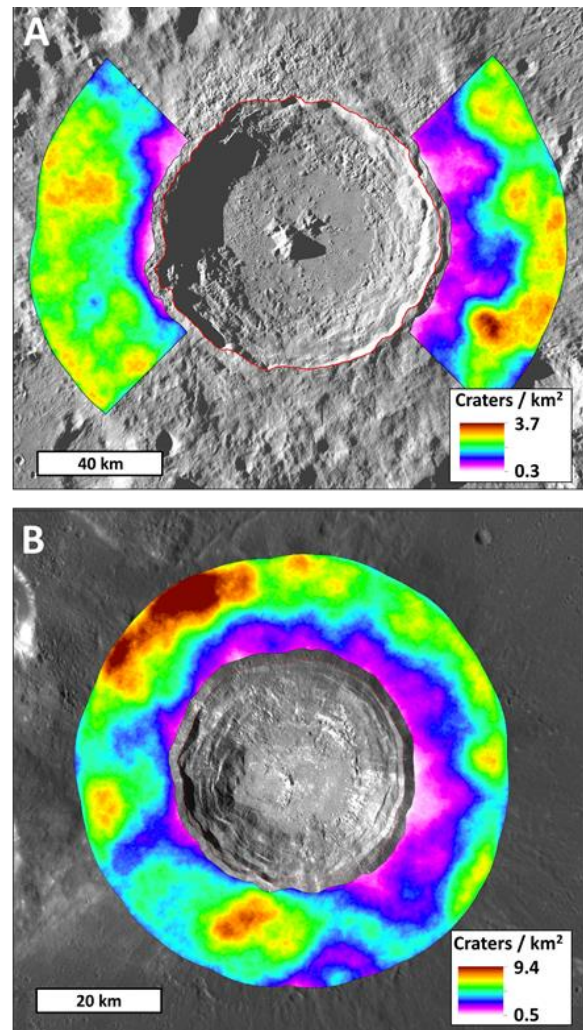


Figure 1: Point Density Maps for a) Tycho and b) Aristarchus Craters. Low density areas are highly correlated with impact melt ponds and flows.

At Aristarchus, similar results are seen, albeit with slightly higher values of craters/ km^2 , owing to the older relative age compared to Tycho (Entire Ejecta: $N(1)=1.47 \times 10^{-4}$, $\text{area}=3.78 \times 10^3$, $\text{AMA}=174 \pm 1.8$) [3]. Again, crater density increases with distance from the

rim (Fig. 1b), and crater density ranges from 0.5 to 9.4 craters/km², with high density regions 4.3 times those of low density regions. Melt-rich areas have low density.

Discussion: It is important to understand the distribution of individual impacts before we can evaluate the effect of other influences on crater SFDs (e.g. target properties, diameter range). The point density distribution of craters records only information about where impacts have occurred, irrespective of crater diameter, which is important because all surfaces were resurfaced at the same and should have the same relative density of craters. Regions of low density are related with impact melt ponds and flows at both Tycho and Aristarchus, suggesting either craters form on impact melt at a slower rate (unlikely), or that impact melt emplacement has erased (auto-secondary) craters that are being recorded elsewhere. Tycho has relatively uniform crater density in the western ejecta, whereas the eastern, melt-rich ejecta show a strong density gradient. Both the uniformity of the western blanket and the broad density gradient of the eastern region can be explained by auto-secondary cratering in the following scenario. The western region received a relatively uniform contribution from auto-secondary projectiles, and only small areas that contain ponded melt have erased the auto-secondary influence. In the eastern region it is plausible that a uniform distribution of auto-secondary craters existed (similar to the western area density), which were then covered by later-arriving impact melt flows. The impact melt covers the auto-secondary craters, which is the final event in the cratering process that resets the surface and begins to record the primary impact crater flux from projectiles in the inner Solar System. Evidence of ghost craters, obscured by impact melt can be seen at some large melt ponds at Tycho, supporting the idea that a pre-existing population of craters on the ejecta blanket existed before the arrival of melt. The proposed SW to NE impactor direction has likely played a role in the distribution of melt in the eastern region, ejecting more melt down-range [13], and may effect auto-secondary distribution as well.

At Aristarchus, the scenario is similar, although it may be that pre-existing topography has played a role in melt distribution rather than parent impactor trajectory. Aristarchus Crater was formed at the boundary of the Aristarchus Plateau, and the western half of the crater formed on a scarp 1km higher than the eastern half (which formed in mare materials). The topographically high regions on the plateau have the highest crater density, while impact melt in the east has the lowest density of craters. The density asymmetry at Aristarchus may be due to different cratering mechanics between the plateau and mare target materials

(where ejection angles may be different for the various materials), but the correlation of impact melt and low density remains [3].

The formation mechanism of auto-secondary craters is still an open question. High angle ejection of ejecta fragments from the parent impact is dynamically difficult [e.g. 18,19]. Ejection velocity must occur below the lunar escape velocity (2.4 km/s), and for material at this velocity to land within the continuous ejecta requires ejection angles of >89.5°. Some high angle ejection is possible if the target is layered with low density, low strength material over high-strength, high density material [18 and references therein], but nearly all experiments and hydrocode models of the cratering process do not predict ejection at angles higher than 70° [e.g. 18, 19]. A recent multi-stage ejection model [20] (which suggests that melt is emplaced outside of crater rims by being thrown up the crater wall and out of the crater in response to the rise of the central peak), offers the potential to deliver blocky material on top of the recently emplaced ejecta, although it is unclear at this time what the ejection angles and velocities might be.

Conclusions: Impact melt surfaces and areas near the rims of Copernican craters are regions of continuous ejecta deposits that are most likely to have recorded a primary population of craters. However, determining SFDs on these surfaces is complicated by target properties, where it is expected that higher strength crystalline melt produces smaller diameter craters than lower strength brecciated ejecta. Our results represent a first step towards estimating the auto-secondary cratering contribution on ejecta blankets. Because the SFD of craters on the ejecta surfaces at Tycho have been used to establish the Copernican impact flux, we must be sure that the best estimate for a primary population of craters is used [9].

References: [1] Shoemaker, E. M. et al. (1962). NASA SP184, 19-128 [2] Oberbeck, V. (1975). Rev of Geophysics 13, 2, 337-362 [3] Zanetti, M. et al (2013), LPSC 44, #1842 [4] Hiesinger, H. et al. (2012), JGR, 117, E2 [5] van der Bogert, C.H. et al. 2010, LPSC 41, #2165 [6] Wuenneman, K. et al. (2012), LPSC 43 #1805 [7] Xaio, B. et al. (2012), Icarus 220, 254-267 [8] McEwen & Bierhaus. (2006). Ann Rev of Earth&Planetary Sci, 32, 535-567 [9] Plescia, J. B. et al. (2012), LPSC 43. #1614. [10] Robinson, M. et al. (2010). Space Sci Rev. 150. 81-124 [11] Haruyama, J. et al. (2008). EPSL, 60, 243-255 [12] Zanetti, M. et al. (2013), LMI-V, #1737 [13] Krüger, T. et al. (2013), LPSC 44, #2152. [14] Kneissl, T. et al. (2010). PSS, 59, 1243-1254 [15] Michael & Neukum. (2010). EPSL, 294, 223-229 [16] Neukum, G. et al. (2001). Space Sci. Review, 96, 55-86 [17] Silverman, B. W. (1986) New York: Chapman and Hall. [18] Schultz, P. et al. (2005), Space Sci Rev 117, 207-239. [19] Collins, G. et al. (2004). Met. & Planetary Sci, 39, 217-231. [20] Osinski, G. et al. (2011). EPSL 310, 167-181.